Geophysical Research Letters

RESEARCH LETTER
10.1029/2018GL080902

Special Section:
The Arctic: An AGU Joint Special Collection

What Caused the Remarkable February 2018 North Greenland Polynya?

G. W. K. Moore[1,2], A. Schweiger[3], J. Zhang[3], and M. Steele[3]

[1]Department of Physics, University of Toronto, Toronto, Ontario, Canada, [2]Department of Chemical and Physical Sciences, University of Toronto Mississauga, Mississauga, Ontario, Canada, [3]Polar Science Center, Applied Physics Laboratory, University of Washington, Seattle, WA, USA

Key Points:
- During late February and early March 2018 a polynya opened off of north Greenland in a region not previously known for polynya formation
- This event occurred after a sudden stratospheric warming that we show was responsible for the conditions that resulted in its development
- We show that the high winds during the event played a dominant role in its formation and sea ice thickness played a less important role

Supporting Information:
- Supporting Information S1

Correspondence to:
G. W. K. Moore,
gwk.moore@utoronto.ca

Citation:
Moore, G. W. K., Schweiger, A., Zhang, J., & Steele, M. (2018). What caused the remarkable February 2018 North Greenland Polynya? *Geophysical Research Letters*, *45*, 13,342–13,350. https://doi.org/10.1029/2018GL080902

Received 1 MAY 2018
Accepted 2 DEC 2018
Accepted article online 6 DEC 2018
Published online 21 DEC 2018

Abstract During late February and early March 2018, an unusual polynya was observed off the north coast of Greenland. This period was also notable for the occurrence of a sudden stratospheric warming. Here we use satellite and in situ data, a reanalysis and an ice-ocean model to document the evolution of the polynya and its synoptic forcing. We show that its magnitude was unprecedented and that it was associated with the transient response to the sudden stratospheric warming leading to anomalous warm southerly flow in north Greenland. Indeed, regional wind speeds and temperatures were the highest during February going back to the 1960s. There is evidence that the thinning sea ice has increased its wind-driven mobility. However, we show that the polynya would have developed under thicker ice conditions representative of the late 1970s and that even with the predicted trend toward thinner sea ice, it will only open during enhanced southerly flow.

Plain Language Summary In late February 2018, satellite imagery revealed the presence of a large polynya (a region of reduced sea ice cover within the pack), in the Wandel Sea off the north coast of Greenland. Since this region is not known for the development of polynyas, this discovery generated interest among Arctic observers and in the science community, raising questions about the nature and cause of this unusual event. In this paper, we show that its opening coincided with a period of sustained and unusually warm winds from the south, with above-freezing temperatures and wind speeds in excess of 25 m/s reported at local weather stations. February 2018 was also notable for a sudden stratospheric warming event, in which an abrupt warming of the atmosphere between 10- and 50-km altitudes occurred in conjunction with a reversal of the stratospheric winds. We show that this event was responsible for the polynya. We also use a computer model to confirm the dominant role of the winds in creating the polynya. Finally, we show that even with future thinning of sea ice due to climate change, extreme winds will remain necessary to create a polynya in this region over the next few decades.

1. Introduction

Media reports indicated that the month of February 2018 was characterized by a period of above-average surface air temperatures in the Arctic (Meyer, 2018; Samenow, 2018). Unlike recent midwinter warmings that had their largest magnitudes to the east of the Greenwich Meridian (Moore, 2016; Rinke et al., 2017), these reports indicated that the warming was centered on north Greenland (Samenow, 2018) and that coincident with it was the development of a polynya over the Wandel Sea (Meyer, 2018), the marginal sea of the Arctic Ocean that lies between the Lincoln Sea to the west and the Fram Strait to the east. This is a region where polynyas have not been previously reported to occur (Barber & Massom, 2007; Morales Maqueda et al., 2004).

During February 2018, media reports also indicated that a sudden stratospheric warming (SSW) event also occurred (Dukes, 2018; Yeginsu, 2018). During such an event, the Northern Hemisphere upper stratosphere undergoes a rapid increase in temperature as well as a collapse of the polar vortex leading to easterly flow that descends to the surface over an ~2-week period (Baldwin & Dunkerton, 2001). A typical SSW lasts for ~20 days, although its impacts on the troposphere can persist for up to ~60 days (Charlton & Polvani, 2007). This time-mean surface response is typically characterized by conditions representative of the negative phase of the North Atlantic Oscillation (NAO), with high pressure over Greenland and the Arctic Ocean and low pressure over southern Europe and the central North Atlantic Ocean (Butler et al., 2017).

In this paper, we document the evolution of the polynya and diagnose the mechanisms responsible for its formation, including the role played by the SSW.

2. Data and Methods

We use sea ice concentration data from the NOAA/NSIDC climate data record, based on the SMMR, SSM/I, and SSMIS instruments at 25-km resolution from 1979 onward (Meier et al., 2014), as well as the University of Bremen's ASI data set, based on the AMSRE and Advanced Microwave Scanning Radiometer 2 instruments at 6.25-km resolution from 2002 onward (Spreen et al., 2008).

The Danish Meteorological Institute (DMI) operates two weather stations in north Greenland (Cappelen, 2018) at Station Nord (SN: 81.6°N; 16.65°W, 1961 to present) and Kap Morris Jessup (83.65°N; 33.37°W, 1985 to present). For the purposes of this paper, the surface pressure, air temperature, wind speed, and wind direction at these stations were sampled every 3 hr throughout their respective periods of operation.

The Pan-Arctic Ice Ocean Modeling and Assimilation System (PIOMAS) will be used to provide information on the processes responsible for the development of the polynya (Zhang & Rothrock, 2003). The standard PIOMAS run (SPINUP) assimilates satellite sea ice concentration and was used to provide initial conditions for the model runs described in this paper (Schweiger et al., 2011). These runs are driven by the NCEP/Reanalysis atmospheric forcing (Kalnay et al., 1996) over the period 1 January to 31 March 2018, with various initial sea ice conditions and forcings. We conducted a control run (CNTRL) and a series of sensitivity runs (Table S1 in the supporting information) for which no data assimilation was performed so as to allow the model to freely evolve without observational constraints, similar to Zhang et al. (2013). Runs were selected to address how the 2018 polynya relates to conditions in the past (when sea ice was thicker and warm air advection was weaker) and in the future (when sea ice is predicted to be thinner). To represent "future ice", we initialized a run with 1 January 2035 sea ice conditions estimated from a run under the IPCC A2 emission scenario (Zhang et al., 2010). The sea ice thickness fields on 1 January 1979, 2018, and 2035 that were used to initialize the various runs are shown in Figure S1, and information on the sea ice thicknesses is provided in Table S1. To test the effect of wind forcing, we reduced surface winds by 25% and 50% from 2018 values during 15 February to 1 March. Finally, to test the effect of the warm temperatures during the polynya opening, we also performed a run with colder thermal forcing from 1979. Table S1 provides information on the differences in surface air temperatures for 1979 and 2018. It should be noted that PIOMAS is not coupled to an atmospheric model and so it will not fully capture the air-sea interactions associated with the evolution of the polynya. In addition, the sensitivity runs are not meant to be an exhaustive sampling of phase space nor predictions of future behavior.

3. Results

3.1. The 2018 analysis

Figure 1 shows the evolution of the February 2018 Wandel Sea polynya as well as placing this event in a longer-term context. On 6 February (Figure 1a), the sea ice concentration in the region was close to 100%. On 16 February (Figure 1b), a flaw lead had developed along the north coast of Greenland midway between the two DMI stations. Rapid expansion into a large polynya subsequently occurred, with it reaching a maximum extent around 25 February (Figure 1c), and by 8 March (Figure 1d) the sea ice concentrations in the region had returned to climatological values. A comparison with observed sea ice concentrations and the PIOMAS SPINUP and CNTRL runs (Figure S2) indicates that the model is able to represent the reduced ice cover associated with the polynya.

Figure 1e shows a gradual increase in polynya size from 16 to 21 February, followed by a rapid expansion to a maximum extent around 25 February; the AMSR2 data set had the maximum opening on the 26th, while the NSIDC CDR and the PIOMAS CNTRL run had it on the 25th. This expansion was followed by a steady reduction in size until its closing on 8 March. The time series of the minimum sea ice concentration in the region of interest during February from the two satellite data sets as well as the PIOMAS CNTRL run are displayed in Figure 1f. Similar results were obtained for other diagnostics. All data sets indicate that previous, smaller, events occurred during February 2011 and 2017. Consideration of the entire winter period, from November to March, confirms the anomalous nature of the February 2018 event (Figure S3). There is

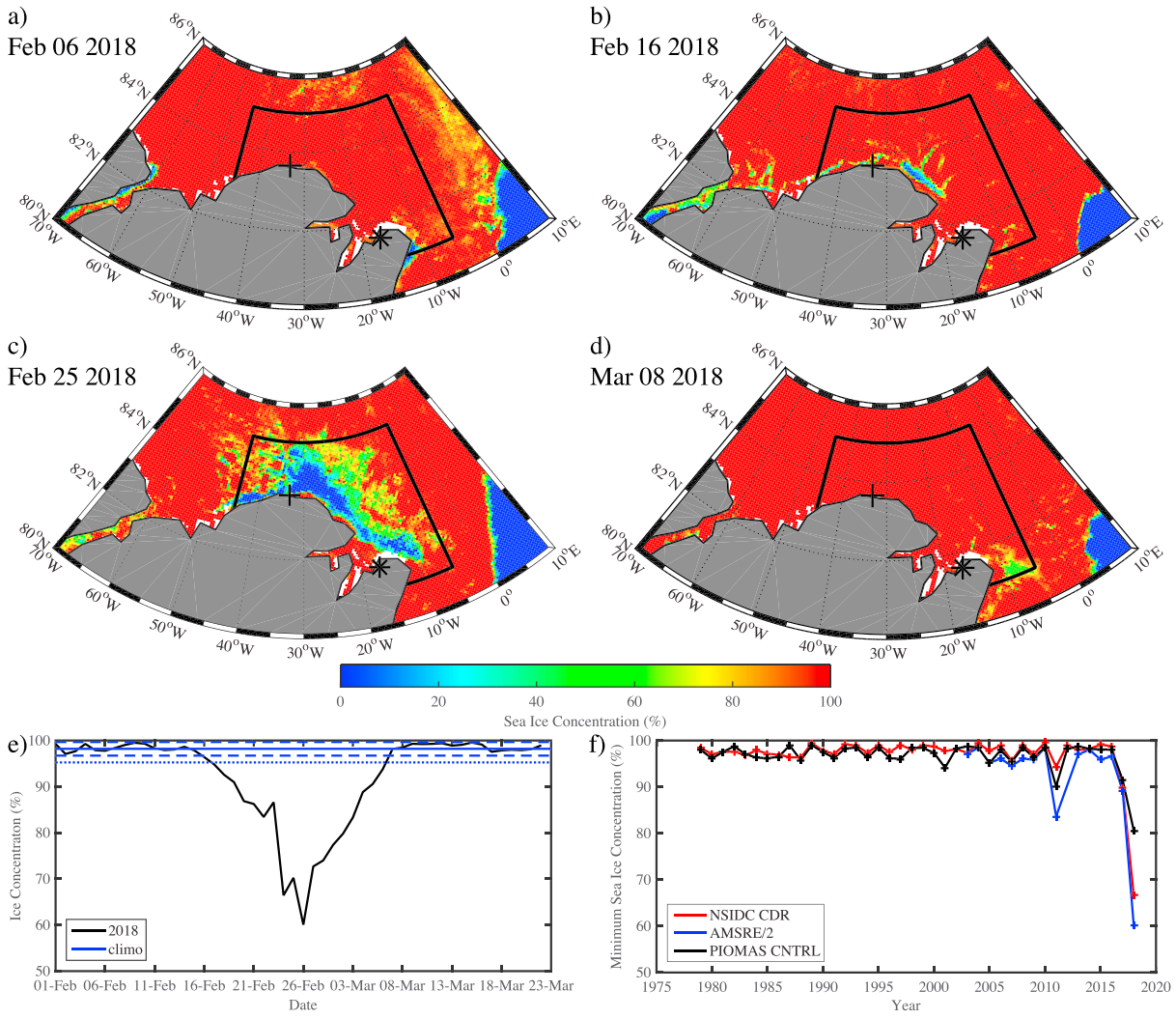

Figure 1. Evolution of the 2018 Wandel Sea polynya. AMSR2 sea ice concentration (%) on (a) 6 February 6, (b) 16 February, (c) 25 February, and (d) 8 March 2018 with the locations of the DMI weather stations at Station Nord and Kap Morris Jesup indicated by the "*" and "+", respectively. (e) Time series of the AMSR sea ice concentration (black curve—%) averaged over the polygon in panels in (a)–(d) and the climatological mean (blue line) with one (blue dotted lines) and two (blue dashed lines) standard deviations above/below the mean. (f) Time series of the minimum sea ice concentration averaged over the polygon in panels (a)–(d) during February for the NSIDC CDR (1979–2018) and the AMSR (2003–2018) data sets as well as the PIOMAS control run. DMI = Danish Meteorological Institute; PIOMAS = Pan-Arctic Ice Ocean Modeling and Assimilation System.

variability among the time series with respect to sea ice concentration in the region that is most likely the result of differences in inputs and the resolution of the two observational data sets (Ivanova et al., 2015) as well as model biases (Schweiger et al., 2011).

Figure 2 shows that typical wind speeds at the two DMI stations in the region (Figure 1) tend to be low, reflective of the region being far from the primary North Atlantic storm track (Moore et al., 2018). Starting around 16 February, air temperatures at the two sites began to increase in association with enhanced southerly flow that was modulated by the passage of two deep cyclones between the 22nd and the 26th. Indeed, during 16 to 26 February, air temperatures at both sites exceeded 0 °C on numerous occasions, multiple standard deviations above the mean. At SN, southerly flow was present during this period with wind speeds in excess of 25 m/s. In fact, these were the highest wind speeds and warmest temperatures ever observed at SN during February since 1961. Wind data at Kap Morris Jessup were not available for the period of the polynya opening.

As noted above, the period of interest was one in which an SSW also occurred. Figure 3a shows the index used to characterize these events, the SSW Index, calculated using the NCEP Reanalysis, defined as the

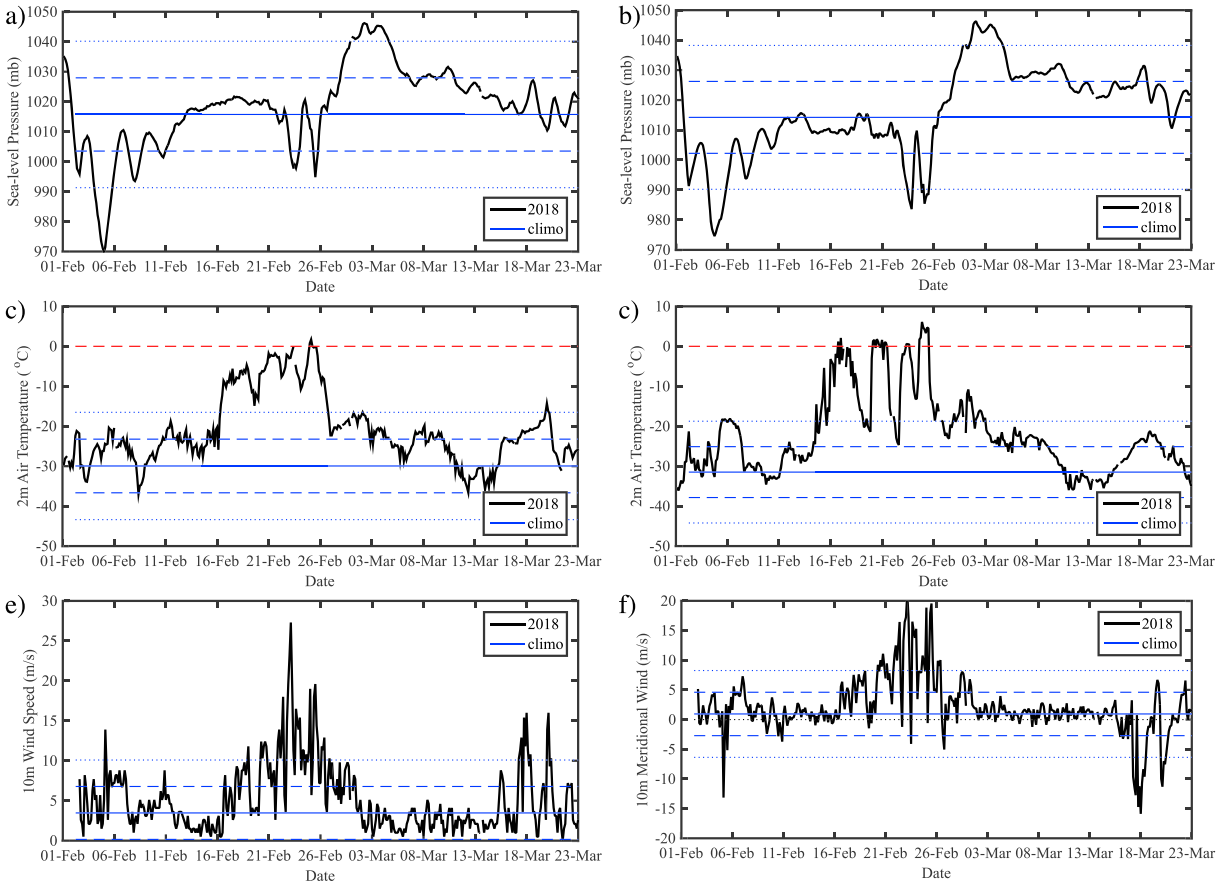

Figure 2. Meteorological observations at Danish Meteorological Institute stations in North Greenland during the evolution of the 2018 Wandel Sea polynya. Time series of the sea level pressure (mb) at (a) Station Nord and (b) Kap Morris Jessup, the 2-m air temperature (°C) at (c) Station Nord and (d) Kap Morris Jessup, the (e) 10-m wind speed (m/s), and (f) the meridional component of the 10-m wind (m/s) at Station Nord. For the 2-m air temperature time series, 0 °C is indicated by the red dashed line. The climatological mean values (blue lines) as well as 1 (dashed blue lines) and 2 (dotted blue lines) standard deviations above and below the mean are also shown. For Station Nord, the climatology is based on 1961–2017, while for Kap Morris Jessup, it is based on 1985–2017.

daily mean zonal mean zonal wind at 60°N and 10 mb (Charlton & Polvani, 2007). The SSW began on 12 February, when this index went negative and persisted through the end of February. A measure of the strength of an SSW, the difference in the area-weighted temperature at 10 mb north of 50°N 5 days after and before the onset of the SSW, exceeded 14 °C during this event. This value is one of the largest for all observed SSWs since 1958 (Charlton & Polvani, 2007; Palmeiro et al., 2015).

Figure 3b shows the NAO Index, also calculated using the NCEP Reanalysis, (Barnston & Livezey, 1987) and indicates that the period of interest was characterized by a transition from NAO positive conditions before 26 February to NAO negative conditions afterward. The lag between the onset of the SSW and its typical surface expression, that is, NAO negative conditions (Kolstad et al., 2010), is reflective of the time it takes the signature of the SSW to propagate from the upper stratosphere to the surface (Baldwin & Dunkerton, 2001).

This evolution of the tropospheric response to this SSW can be seen in Figures 3c–3f which show meridional height cross sections of the geopotential height and temperature anomalies along 80°N. On 9 February 2018, prior to the onset of SSW, it indicates that negative height anomalies were present throughout the atmosphere west of 45°W (Figure 3c). After its onset on 12 February 2018, there was a warming of the stratosphere to the east of 45°W that was associated with positive height anomalies (Figure 3d). Over the next 2 weeks, this height anomaly descended toward the surface (Baldwin & Dunkerton, 2001). On 25 February 2018, the descent of the SSW anomaly along with the preexisting negative height anomalies over the western Arctic resulted in a surface meridional pressure gradient in the vicinity of north Greenland and a surface trapped warming (Figure 3e). By early March 2018, positive height anomalies, consistent with the observed NAO negative conditions, were present in the vicinity of north Greenland (Figure 3f).

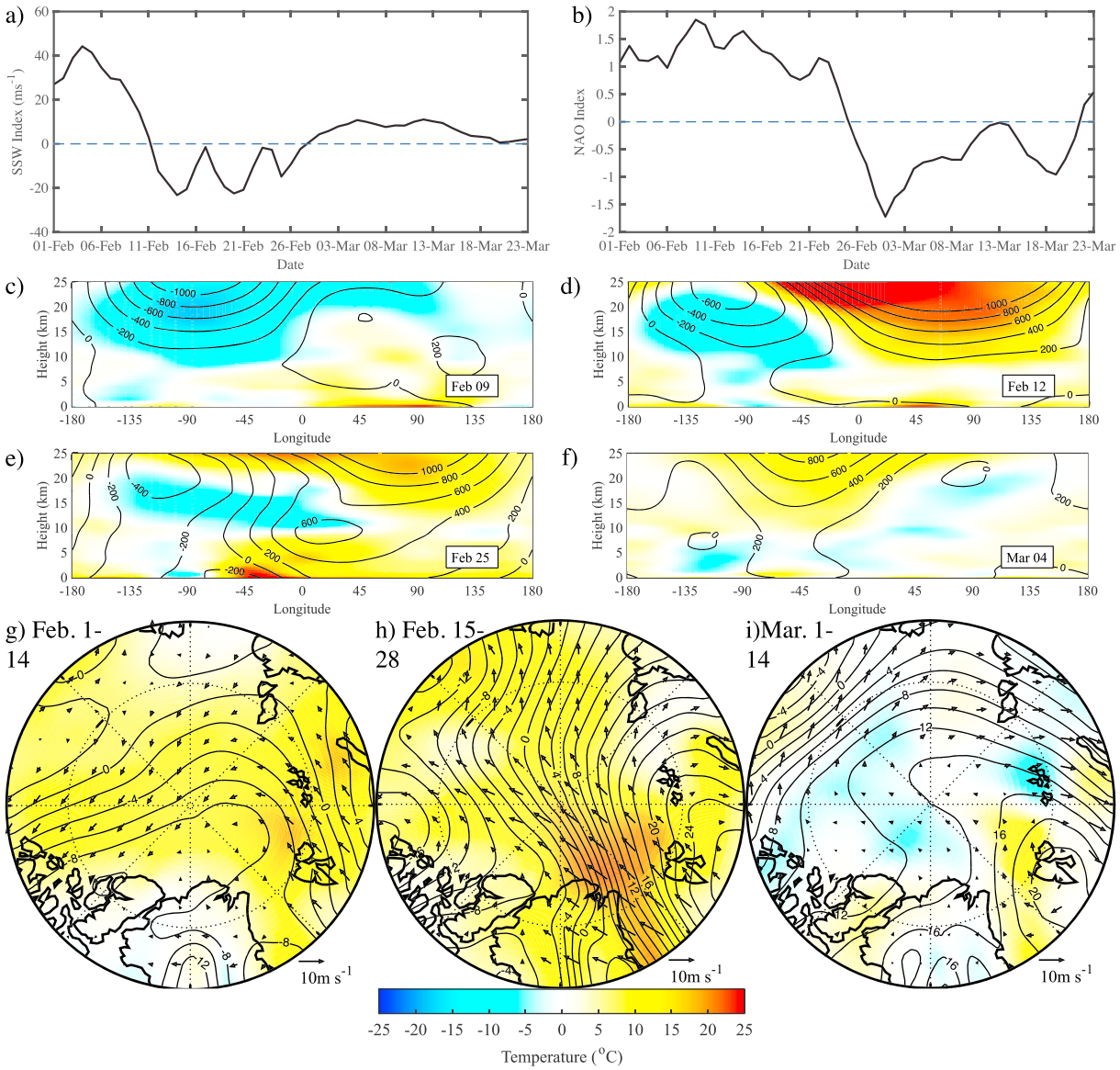

Figure 3. Spatial and temporal variability in the meteorology during the 2018 Wandel Sea polynya. Time series of (a) the sudden stratospheric warming index (m/s) and (b) the NAO index. Meridional-height anomalies in the geopotential height (m—contours) and temperature (°C—shading) along 80°N on (c) 9 February, (d) 12 February, (e) 25 February, and (f) 4 March 2018. Sea level pressure (mb—contours), 2-m air temperature (°C—shading), and 10-m wind (m/s—vector) anomalies during (g) the first half of February 2018, (h) the second half of February 2018, and (i) the first half of March 2018. All data are based on the NCEP Reanalysis. The anomalies are based on the years1948–2017.

This transient response at the surface can be seen more clearly in Figures 3g–3i. During the first half of February, there were anomalously low sea level pressures in the vicinity of Iceland and Greenland that, along with a region of high pressure over the southern Barents Sea, resulted in enhanced southerly flow toward Spitzbergen (Figure 3g). This led to anomalously warm surface air temperatures over the northern Barents Sea. During the second half of February, the region of high pressure, which was associated with the SSW, moved westward and strengthened (Figure 3h). This anomaly, along with continued low pressures over the eastern Arctic, resulted in a strong meridional pressure gradient along the east coast of Greenland that led to enhanced warm southerly flow observed at the DMI stations (Figure 2). By the first half of March, the situation was similar to the typical surface response to a SSW with high pressure, that is, NAO negative conditions, extending across subpolar North Atlantic and Greenland regions (Figure 3i).

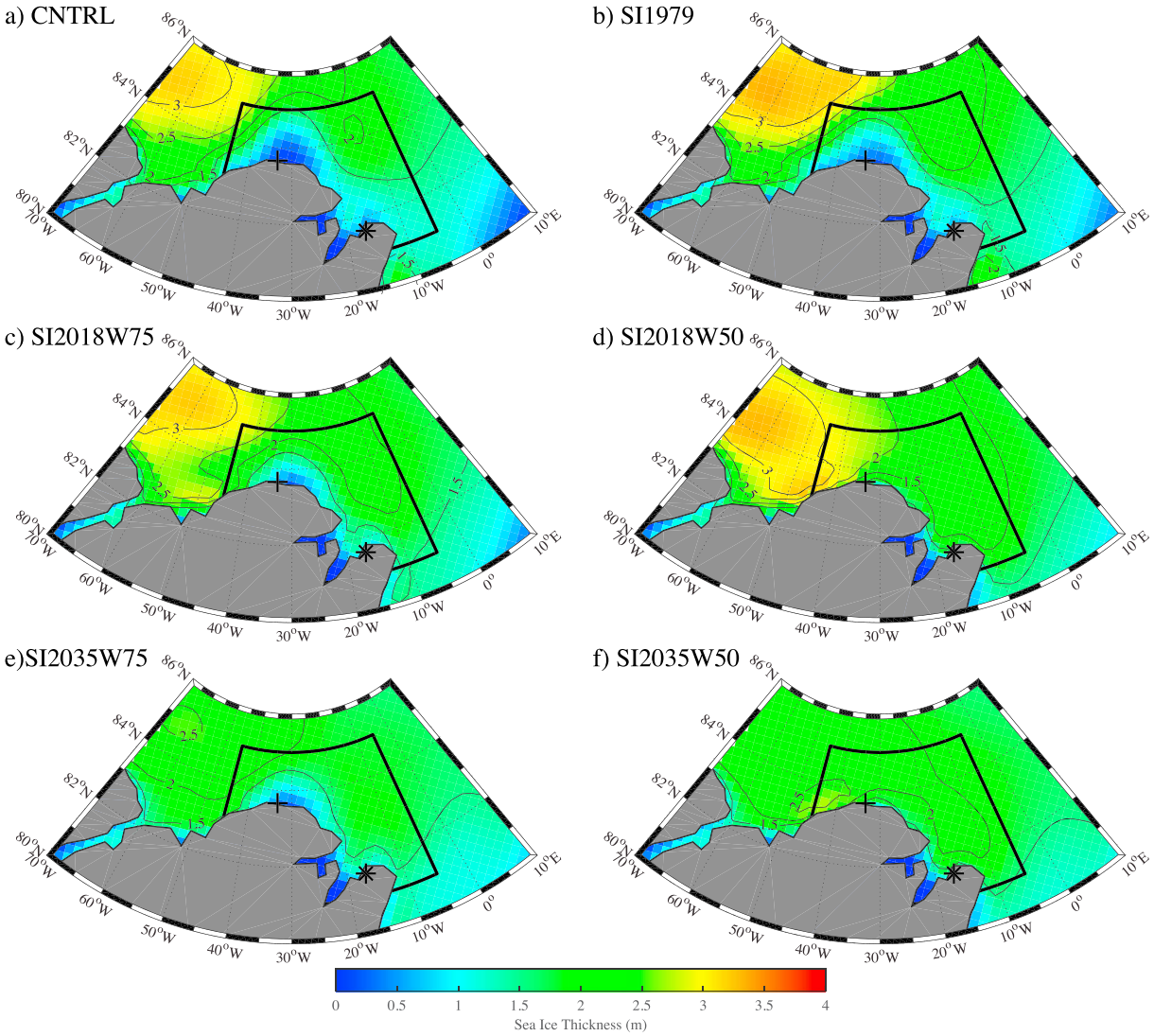

Figure 4. Structure of the 2018 North Greenland Polynya as represented in PIOMAS. The sea ice thickness (m) on 25 February 2018 for (a) the control run, (b) the sensitivity run initialized with sea ice thickness from 1 January 1979, (c) the sensitivity run with winds during the second half of February reduced by 25%, (d) the sensitivity run with winds during the second half of February reduced by 50%, (e) the sensitivity run with sea ice thickness from 1 January 2035 and winds during the second half of February reduced by 25%, and (f) the sensitivity run with sea ice thickness from 1 January 2035 and winds during the second half of February reduced by 50%.

3.2. Sensitivity Experiments

Would this polynya have occurred if sea ice was still as thick as it was in 1979? Will future thinning of sea ice make it more likely for this polynya to occur, even under less extreme wind forcing? What was the role of warm air advection in the development of the polynya?

Figure 4 shows the sea ice thickness on the date of maximum polynya extent (i.e., 25 February 2018) from the CNTRL and five sensitivity runs. The CNTRL run, Figure 4a, clearly shows the development of a region of reduced sea ice thickness over the Wandel Sea in the same region as the observed polynya (Figure 1). When the initial 1 January ice thickness is increased to 1979 values, Figure 4b, we also see a development of a smaller polynya with thicker sea ice as compared to CNTRL. With 2018 sea ice conditions, reducing the wind speeds during the second half of February by 25%, Figure 4c, still results in a polynya (albeit smaller in size than for the CNTRL run), while a reduction to 50% of the original wind speed, Figure 4d, shows only minor changes in the region of interest. On the other hand, reducing the initial 1 January ice thickness to 2035 values had little effect on polynya formation as compared to the 2018 runs (Figures 4e and 4f).

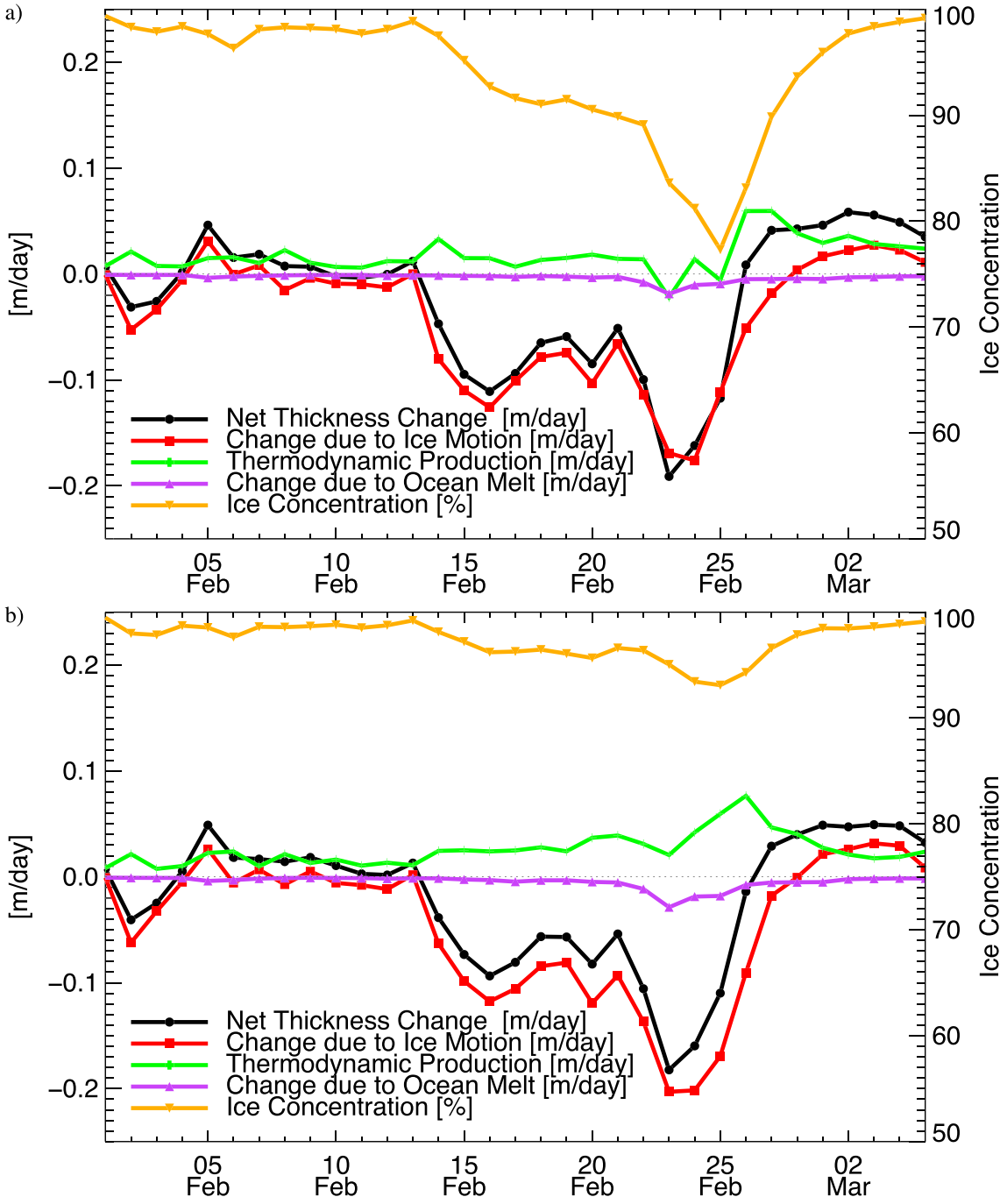

Figure 5. Pan-Arctic Ice Ocean Modeling and Assimilation System sea ice concentration (%) and sea ice thickness budget (m/day) during the period 1 February to 5 March 2018 over the region of interest for (a) the control run and (b) the sensitivity run with 1979 thermal conditions.

Figure 5 shows the time series of the sea ice concentration as well as the sea ice thickness budget (Zhang et al., 2008) from the CNTRL run and the sensitivity run using 1979 thermal forcing. The CNTRL run, Figure 5a, shows polynya size slowly increasing starting on 11 February and then more rapidly ~9 days later, with maximum extent on 25 February and then a steady reduction to closing in early March. This evolution is consistent with that of the observed polynya, Figure 1e, with the differences attributable to resolution, satellite retrieval issues, and/or model biases. The thickness budget shows that the change was due to ice motion in response to the wind forcing was the largest contributor to the polynya formation even as ice production

occurred throughout the period. There was also some ice melt due to entrainment of ocean heat from below the mixed layer, driven by local winds and ice growth and enhanced by upwelling (Figure S4). With 1979 thermal forcing that represents a mean surface air temperature during the period of interest of −38 °C as compared to −10 °C during 2018, Figure 5b, the polynya had a similar evolution to the CNTRL run, albeit with higher sea ice concentrations as compared to the CNTRL run. The reason for this can be seen in the enhanced ice production due to colder surface air temperatures and enhanced loss of heat to the atmosphere.

4. Discussion

Late February to early March 2018 was remarkable for the occurrence of a polynya in the Wandel Sea off the coast of north Greenland in a region not previously recognized for such events (Figure 1). We have shown that the period of its opening coincided with a period of sustained anomalously warm southerly flow that resulted in above freezing temperatures and wind speeds in excess of 25 m/s at local weather stations (Figure 2). This is different from the recently observed transient North Pole minwinter warmings (Moore, 2016; Rinke et al., 2017). February 2018 was also notable for the SSW that began on the 12th. We have shown that the transient surface response to this event was responsible for the high winds and warm temperatures during the period of the polynya's opening with the period of its closing associated with the transition to NAO negative conditions characterized by colder temperatures and weaker winds (Figures 2 and 3).

There is evidence that previously unreported polynyas in the region have formed during previous winters (Figures 1f and S3). However, the February 2018 event was significantly larger than these other events. The previous events were also associated with enhanced southerly flow but not with the occurrence of SSWs (Figure S5). This is consistent with the PIOMAS ice thickness budget that indicates the polynya was the result of divergent sea ice motion (Figure 5).

The PIOMAS model was able to represent the evolution of the polynya with the caveat that in the CNTRL run, it was smaller than observed (Figure S1). The sensitivity runs show that it was the high winds that were primarily responsible for the opening of the polynya (Figures 4 and 5). The warmer surface air temperatures during the second half of February 2018 also contributed by reducing sea ice production. Once the wind forcing was removed, the polynya rapidly closed.

Even under past conditions with considerably thicker sea ice, we find that the polynya would have still formed (Figure 4b). Model runs with future sea ice thickness show that for the foreseeable future, wind forcing will play a dominant role in polynya formation in this region (Figures 4e and 4f). This means that thinner sea ice will not in and of itself result in more frequent polynya formation, a result of two factors. First, the Wandel Sea is a region where future reduction in sea ice may be modest (Figure S1 and Table S1). Second, the region surrounding the Wandel Sea is characterized by thick ice that tends to inhibit the advection of sea ice away from the polynya. While the fact that sea ice remains relatively thick in this area is consistent with the pattern of ice motion, this conclusion maybe model and scenario dependent.

Acknowledgments
The authors would like to acknowledge the NSIDC and the University of Bergen for access to the sea ice concentration data, the Danish Meteorological Institute for access to the automatic weather station data, the NOAA/ESRL for access to the NCEP reanalysis data, and NASA for access to the Suomi satellite data. PIOMAS data are available from the Polar Sciences Center at the University of Washington. G. W. K. M. would like to acknowledge funding from the Natural Sciences and Engineering Research Council of Canada. A. S. was supported by ONR grant N00014-17-1-3162, NSF grant ARC-1203425, and NOAA grant NA15OAR4310162. J. Z. was supported by NASA grants NNX17AD27G and NNX15AG68G and NSF grants PLR-1416920 and PLR-1603259. M. S. was supported by NSF grants OCE-1233255 and ARC-1203506 and ONR grant N00014-17-1-2545.

References

Baldwin, M. P., & Dunkerton, T. J. (2001). Stratospheric harbingers of anomalous weather regimes. *Science*, *294*(5542), 581–584. https://doi.org/10.1126/science.1063315

Barber, D. G., & Massom, R. A. (2007). The role of sea ice in Arctic and Antarctic polynyas. *Elsevier Oceanography Series*, *74*, 1–54. https://doi.org/10.1016/S0422-9894(06)74001-6

Barnston, A. G., & Livezey, R. E. (1987). Classification, seasonality and persistence of low-frequency atmospheric circulation patterns. *Monthly Weather Review*, *115*(6), 1083–1126. https://doi.org/10.1175/1520-0493(1987)115<1083:CSAPOL>2.0.CO;2

Butler, A. H., Sjoberg, J. P., Seidel, D. J., & Rosenlof, K. H. (2017). A sudden stratospheric warming compendium. *Earth System Science Data*, *9*(1), 63–76. https://doi.org/10.5194/essd-9-63-2017

Cappelen, J. (2018). Weather observations from Greenland 1958–2017. Observation data with description. DMI Report 18-08. Copenhagen, https://doi.org/10.3233/978-1-61499-923-2-634

Charlton, A. J., & Polvani, L. M. (2007). A new look at stratospheric sudden warmings. Part I: Climatology and modeling benchmarks. *Journal of Climate*, *20*(3), 449–469. https://doi.org/10.1175/JCLI3996.1

Dukes, M. (2018). Weatherwatch: Sudden stratospheric warming and the beast from the east. The Guardian. Retrieved from https://www.theguardian.com/news/2018/mar/19/weatherwatch-sudden-stratospheric-warming-beast-from-the-east, https://doi.org/10.1111/biom.12943

Ivanova, N., Pedersen, L., Tonboe, R., Kern, S., Heygster, G., Lavergne, T., Sørensen, A., et al. (2015). Inter-comparison and evaluation of sea ice algorithms: Towards further identification of challenges and optimal approach using passive microwave observations. *The Cryosphere*, *9*(5), 1797–1817. https://doi.org/10.5194/tc-9-1797-2015

Kalnay, E., Kanamitsu, M., Kistler, R., Collins, W., Deaven, D., Gandin, L., Iredell, M., et al. (1996). The NCEP/NCAR 40-year reanalysis project. *Bulletin of the American Meteorological Society*, *77*(3), 437–471. https://doi.org/10.1175/1520-0477(1996)077<0437:TNYRP>2.0.CO;2

Kolstad, E. W., Breiteig, T., & Scaife, A. A. (2010). The association between stratospheric weak polar vortex events and cold air outbreaks in the Northern Hemisphere. *Quarterly Journal of the Royal Meteorological Society*, *136*(649), 886–893. https://doi.org/10.1002/qj.620

Meier, W. N., Peng, G., Scott, D. J., & Savoie, M. H. (2014). Verification of a new NOAA/NSIDC passive microwave sea-ice concentration climate record. *Polar Research*, *33*(1), 21004. https://doi.org/10.3402/polar.v33.21004

Meyer, R. (2018). Parts of the Arctic spiked to 45 degrees above normal. *The Atlantic Monthly*.

Moore, G. W. K. (2016). The December 2015 North Pole warming event and the increasing occurrence of such events. *Scientific Reports*, *6*, 39084. https://doi.org/10.1038/srep39084

Moore, G. W. K., Schweiger, A., Zhang, J., & Steele, M. (2018). Collapse of the 2017 winter Beaufort High: A response to thinning sea ice? *Geophysical Research Letters*, *45*(6), 2860–2869. https://doi.org/10.1002/2017GL076446

Morales Maqueda, M. A., Willmott, A. J., & Biggs, N. R. T. (2004). Polynya dynamics: A review of observations and modeling. *Reviews of Geophysics*, *42*, RG1004. https://doi.org/10.1029/2002RG000116

Palmeiro, F. M., Barriopedro, D., García-Herrera, R., & Calvo, N. (2015). Comparing sudden stratospheric warming definitions in reanalysis data. *Journal of Climate*, *28*(17), 6823–6840. https://doi.org/10.1175/JCLI-D-15-0004.1

Rinke, A., Maturilli, M., Graham, R. M., Matthes, H., Handorf, D., Cohen, L., et al. (2017). Extreme cyclone events in the Arctic: Wintertime variability and trends. *Environmental Research Letters*, *12*(9), 094006. https://doi.org/10.1088/1748-9326/aa7def

Samenow, J. (2018). North Pole surges above freezing in the dead of winter, stunning scientists. The Washington Post. Retrieved from https://www.washingtonpost.com/news/capital-weather-gang/wp/2018/02/26/north-pole-surges-above-freezing-in-the-dead-of-winter-stunning-scientists/?noredirect=on&utm_term=.1f38cb3298b7

Schweiger, A., Lindsay, R., Zhang, J., Steele, M., Stern, H., & Kwok, R. (2011). Uncertainty in modeled Arctic sea ice volume. *Journal of Geophysical Research*, *116*, C00D06. https://doi.org/10.1029/2011JC007084

Spreen, G., Kaleschke, L., & Heygster, G. (2008). Sea ice remote sensing using AMSR-E 89-GHz channels. *Journal of Geophysical Research*, *113*, C02S03. https://doi.org/10.1029/2005JC003384

Yeginsu, C. (2018). Heaviest snow in decades Batters U.K., Ireland and the Continent. New York Times. https://doi.org/10.21470/1678-9741-2018-0126

Zhang, J., Lindsay, R., Schweiger, A., & Steele, M. (2013). The impact of an intense summer cyclone on 2012 Arctic Sea ice retreat. *Geophysical Research Letters*, *40*, 720–726. https://doi.org/10.1002/grl.50190

Zhang, J., Lindsay, R., Steele, M., & Schweiger, A. (2008). What drove the dramatic retreat of arctic sea ice during summer 2007? *Geophysical Research Letters*, *35*, L11505. https://doi.org/10.1029/2008GL034005

Zhang, J., & Rothrock, D. A. (2003). Modeling global sea ice with a thickness and enthalpy distribution model in generalized curvilinear coordinates. *Monthly Weather Review*, *131*(5), 845–861. https://doi.org/10.1175/1520-0493(2003)131<0845:MGSIWA>2.0.CO;2

Zhang, J., Steele, M., & Schweiger, A. (2010). Arctic sea ice response to atmospheric forcings with varying levels of anthropogenic warming and climate variability. *Geophysical Research Letters*, *37*, L20505. https://doi.org/10.1029/2010GL044988